nature chemical biology

ARTICLE

PUBLISHED ONLINE: 28 APRIL 2014 | DOI: 10.1038/NCHEMBIO.1522

The voltage-gated sodium channel TPC1 confers endolysosomal excitability

Chunlei Cang*, Biruk Bekele & Dejian Ren*

The physiological function and molecular regulation of plasma membrane potential have been extensively studied, but how intracellular organelles sense and control membrane potential is not well understood. Using whole-organelle patch clamp recording, we show that endosomes and lysosomes are electrically excitable organelles. In a subpopulation of endolysosomes, a brief electrical stimulus elicits a prolonged membrane potential depolarization spike. The organelles have a previously uncharacterized, depolarization-activated, noninactivating Na^+ channel (lysoNa$_V$). The channel is formed by a two-repeat six-transmembrane-spanning (2×6TM) protein, TPC1, which represents the evolutionary transition between 6TM and 4×6TM voltage-gated channels. Luminal alkalization also opens lysoNa$_V$ by markedly shifting the channel's voltage dependence of activation toward hyperpolarization. Thus, TPC1 is a member of a new family of voltage-gated Na^+ channels that senses pH changes and confers electrical excitability to organelles.

© 2014 Nature America, Inc. All rights reserved.

Electrical potential differences exist across the lipid bilayers of plasma membranes and intracellular organelles in all cells[1]. The biological functions and molecular mechanisms underlying the generation and regulation of plasma membrane potential (V_m) have been extensively studied[1,2]. V_m controls cellular processes such as ion transport, secretion, membrane fusion, fertilization, muscle contraction and nerve communication. By facilitating ion movement across the plasma membrane, ion channels and pumps are fundamental determinants of V_m. In addition, voltage-gated ion channels are also the major targets of V_m. During action potentials in the neurons, for example, V_m depolarization opens both voltage-gated Na^+ (Na_V) and voltage-gated K^+ (K_V) channels[2].

Studies using electrophysiological methods and molecular cloning have discovered several hundred plasma membrane ion channel proteins (reviewed in refs. 1,3). In bacteria, 6TM proteins form Na_Vs[4], whereas in animals, 4×6TM proteins form Na_Vs[5,6]. It is not known whether 2×6TM proteins, the evolutionary transition between the 6TM and 4×6TM proteins, are able to form Na_Vs.

The 2×6TM channel family in animals contains three members (TPC1–TPC3). A functional *tpc3* gene is found in some animals, such as cats and dogs, but not in humans or mice[7–9]. The biophysical properties of TPCs and their activators are not well understood because their primary localization is in intracellular organelles, which are less accessible to electrophysiological characterization. Some studies have suggested that TPCs are Ca^{2+}-permeable channels activated by nicotinic acid adenine dinucleotide phosphate (NAADP)[10–16]. NAADP does not bind TPC proteins in photoaffinity labeling assays[17,18]. In addition, whole-organelle recordings of enlarged lysosomes suggest that TPC1 (this study) and TPC2 (refs. 19,20) are highly Na^+ selective. Therefore, whether NAADP activates Ca^{2+} release directly through TPC channels *in vivo* requires further validation. To achieve maximal TPC channel activation, phosphatidylinositol bisphosphate (PI(3,5)P2) is required[19]. It is not clear whether physiological levels of PI(3,5)P2 are required for basal channel activity in the way that many plasma membrane ion channels require PI(4,5)P2 (refs. 21,22) or whether changes in PI(3,5)P2 levels during signaling activate TPCs. In addition, TPC currents are also activated by decreases in intracellular ATP concentration and by depletion of extracellular amino acids via a mechanistic target of rapamycin (mTOR)-dependent mechanism[20].

Previous studies using voltage-sensitive reporter molecules[23,24] and direct current-clamp electrophysiological recordings[20] have shown that the membrane potentials (Ψ) of endosomes and lysosomes change in response to physiological stimuli, such as ATP concentration. However, in contrast to our understanding of plasma membranes, how intracellular organelles control Ψ at the molecular level is poorly understood. Many ion channel and transporter proteins, such as members of the CLC family of Cl^-/H^+ exchangers and $Na_V1.5$, a member of the 4×6TM Na_V family, have been detected in endolysosomes[25,26]. In addition, TTX (a Na_V blocker) and veratridine (a Na_V activator) affect lumen pH and Na^+ content of endosomes in human macrophages when applied at high concentrations[26]. The whole-endolysosomal electrophysiological properties of these proteins have not been well characterized. Similarly, whether there are endosome- or lysosome-specific Na_V and K_V channels is not known. Finally, how endolysosomes detect and control luminal pH, which changes markedly from endosomes (pH ~6) to lysosomes (pH ~4), is also not well understood[25,27].

Here, we report a new voltage-gated, noninactivating Na^+ channel, which we call lysoNa$_V$, whose activity is recorded from whole endolysosomes. LysoNa$_V$ is formed by TPC1 but not by TPC2. Luminal alkalization also opens TPC1 by shifting the channel's voltage dependence of activation toward hyperpolarization. Furthermore, in endolysosomes with TPC1 but not in those without it, a brief electrical stimulus leads to a long-lasting depolarization spike. Thus, endolysosomes sense both voltage and pH changes with lysoNa$_V$. The organelles can be classified as excitable and nonexcitable, depending on the level of expression of the atypical voltage-gated Na^+ channel.

RESULTS

Whole-endolysosomal K^+, Na^+, H^+ and Cl^- permeabilities

The ionic conductance of plasma membranes has been extensively studied since the 1940s (ref. 2), but similar systematic studies have not been performed in endolysosomes owing to the technical difficulties associated with performing whole-organelle electrophysiological recordings. To determine the ionic permeability of endolysosomal membranes, we performed whole-organelle current- and voltage-clamp recordings on enlarged endolysosomes excised from cells by cutting the plasma membrane with a glass pipette tip[28–30].

Department of Biology, University of Pennsylvania, Philadelphia, Pennsylvania, USA. *e-mail: ccang@sas.upenn.edu or dren@sas.upenn.edu

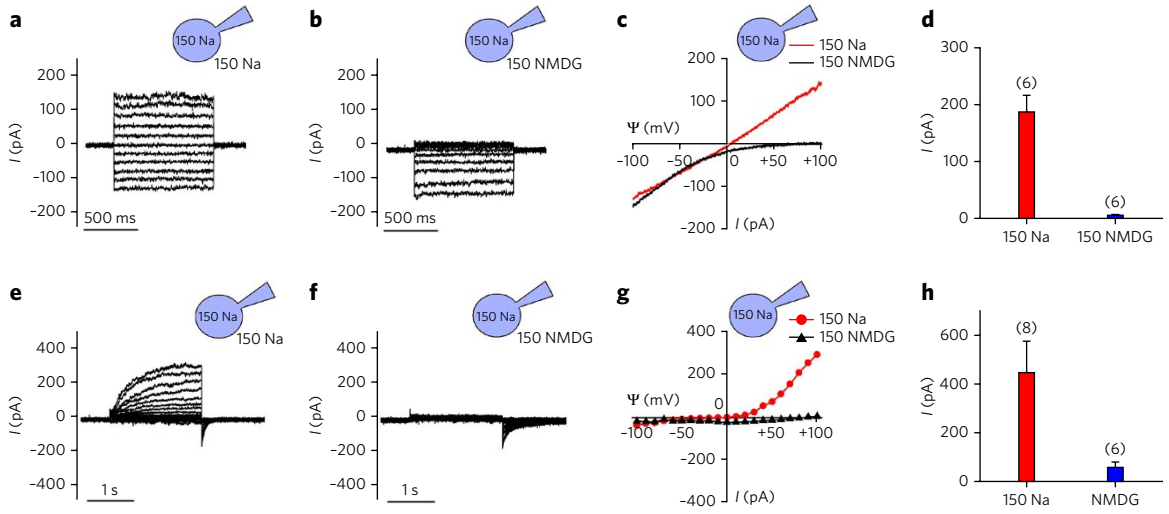

Figure 1 | A new organellar voltage-gated Na⁺ channel. (**a**–**h**) Na^+ currents were recorded from endolysosomes isolated from macrophages (**a**–**d**) and contracting cardiac myocytes (**e**–**h**). Panels **a** and **e** show recordings with Na^+-containing baths (1 mM HCl, 150 mM Na^+, 1 μM PI(3,5)P2, 10 mM HEPES, pH 7.2, with methanesulfonic acid). Panels **b** and **f** show recordings with baths containing no Na^+ (replaced with NMDG). Panels **c** and **g** show I-Ψ relationships obtained using a ramp protocol (in **c**, -100 mV to +100 mV in 1 s, V_h = 0 mV) or reconstructed (in **g**) from the currents in **e** and **f** (measured at the end of the pulse steps). Panels **d** and **h** show averaged current amplitudes (at +100 mV in **d** and +150 mV in **h**). Step protocols were used in **a**, **b**, **e** and **f** (in **a** and **b**, step of 20 mV, V_h = 0 mV; in **e** and **f**, step of 10 mV, V_h = -70 mV). The pipette solution contained 1 mM HCl, 150 mM Na^+ and 10 mM MES (pH 4.6, adjusted with methanesulfonic acid). Ψ is the membrane potential (defined as $V_{cytosol} - V_{lumen}$ (ref. 50)). Inward current (negative) denotes flow of positive charges into the cytosol (bath) from the lumen (pipette). Numbers of endolysosomes are in parentheses. Data are represented as mean ± s.e.m.

In endolysosomes from mouse peritoneal macrophages, we detected K^+ currents (**Supplementary Results**, **Supplementary Fig. 1a**). The current-voltage (I-Ψ) relationship was largely linear, suggesting that the underlying K^+ conductance is voltage independent. On plasma membranes, similar voltage-independent, leak-like conductances are formed by members of the K2P K^+ leak channel family[31]. K2P proteins are also found on endosomes and may have produced the K^+-leak conductance that we detected[32]. Plasma membranes also have more than 40 K_Vs[2,33]. To our surprise, we did not record K_V activity in endolysosomes from macrophages (**Supplementary Fig. 1a**; n = 5), contracting cardiac myocytes (n = 9) or mIMCD3 kidney cells (n = 9).

Endolysosomal membranes are highly permeable to H^+ (P_H/P_K = 7,185 ± 720; mean ± s.e.m., n = 5 macrophage endolysosomes) and have H^+ conductance (**Supplementary Fig. 1b**). We also recorded Cl^- currents from macrophage (**Supplementary Fig. 1c**) and cardiac myocyte endolysosomes. Removing Cl^- from the pipette (lumen) abolished the current (**Supplementary Fig. 1c**), suggesting that the underlying conductance allows Cl^- to move unidirectionally from the organelle lumen to cytosol (outwardly rectifying). Several CLC H^+/Cl^- exchange proteins are localized on endolysosomal membranes and, when misexpressed on plasma membranes, have properties similar to the recordings from endolysosomes[25,27,34,35]. It remains to be determined whether CLCs and other known Cl^- and H^+ channels are responsible for the endolysosomal H^+/Cl^- conductances we detected.

The membrane potentials of the organelles changed substantially under current clamp recordings with different cytosolic compositions (1 mM ATP, no PI(3,5)P2: −12.8 ± 5.4 mV with 150 mM KCl, 31.3 ± 10.9 mV with 150 mM NaCl, n = 6; no ATP, 0.1 μM PI(3,5)P2: +2.6 ± 2.4 mV with 150 mM KCl, −44.2 ± 7.0 mV with 150 mM NaCl, n = 5). We used the membrane potentials to estimate the relative Na^+ permeability (P_{Na}/P_K) of endolysosomal membranes. P_{Na}/P_K was increased 28-fold by $PI(3,5)P_2$ (P_{Na}/P_K = 0.31 ± 0.1 in bath containing no $PI(3,5)P_2$ or ATP, n = 6; 8.7 ± 3.3 in bath containing 0.1 μM $PI(3,5)P_2$, n = 5 macrophage endolysosomes).

A voltage-gated Na^+ channel in endolysosomes

To uncover the ionic conductances underlying the Na^+ permeabilities, we used bath and pipette solutions containing Na^+ as the major cation and a step voltage protocol. Our results revealed voltage-independent and voltage-dependent Na^+ conductances. In macrophage endolysosomes, the Na^+ conductance was largely voltage-independent, as demonstrated by the linear I-Ψ relationship (**Fig. 1a–d**). Similar voltage-independent conductances were also recorded from contracting cardiac myocytes.

Remarkably, depolarization above 0 mV elicited voltage-dependent Na^+ conductances in a subpopulation of endolysosomes from cardiac myocytes (26 out of 31; **Fig. 1e–h**) and nonexcitable kidney cells (22 out of 29; **Supplementary Fig. 2**). The channel opened slowly (for cardiac myocytes, τ at +150 mV was 204 ± 25 ms, n = 23, and τ at +100 mV was 424 ± 67 ms, n = 20; for kidney cells, τ at +150 mV was 646 ± 76 ms, n = 12, and τ at +100 mV was 1,392 ± 473 ms, n = 11) and did not inactivate. The channel also closed slowly, which was illustrated by the slowly deactivating tail currents upon repolarization (τ of tail currents from +150-mV pulses: cardiac myocytes, 76 ± 7 ms, n = 23; kidney cells, 75 ± 7 ms, n = 12; from +100-mV pulses: cardiac myocytes, 75 ± 8 ms, n = 20; kidney cells, 103 ± 12 ms, n = 11). Thus, a subpopulation of endolysosomes in both excitable and nonexcitable cells have lysoNa$_V$s.

TPC1 forms a lysoNa$_V$-like voltage-gated channel

To determine the molecular identity of lysoNa$_V$s, we tested whether candidate proteins formed lysoNa$_V$-like channels when transfected into HEK293 cells, which have no detectable endogenous lysoNa$_V$ currents ($I_{lysoNaV}$; **Fig. 2a**). LysoNa$_V$'s biophysical properties, including its slow activation, deactivation and lack of inactivation, are unlike those of any of the Na$_V$s, including the fast-inactivating Na$_V$1.5. We then tested whether the 2×6TM TPC proteins formed lysoNa$_V$s. Previous whole-endolysosome TPC recordings by us and others used ramp voltage protocols with asymmetric Na^+ concentrations in the cytosol and lumen, which most likely masked the voltage dependence of channel activation[19,20,36]. When recorded with symmetrical

© 2014 Nature America, Inc. All rights reserved.

Na^+ concentrations (145 mM in both lumen and cytosol) using a voltage step protocol, TPC2 showed a conductance with a largely linear I-Ψ relationship between −100 mV and +100 mV (**Fig. 2b**), suggesting that TPC2 formed a voltage-independent leak-like channel similar to that recorded in macrophage endolysosomes (**Fig. 1a–c**).

Remarkably, transfection of TPC1 generated large currents when Ψ was depolarized (**Fig. 2c**). Like the cardiac myocyte and kidney cell lysoNa$_V$s (**Fig. 1e–g** and **Supplementary Fig. 2**), TPC1 activated slowly ($\tau = 416 \pm 51$ ms at +150 mV and 450 ± 51 ms at +100 mV, $n = 21$) and had slowly deactivating tail currents (τ of tail currents from +150-mV pulses: 103 ± 13 ms; from +100-mV pulses: 94 ± 11 ms; $n = 16$). In addition, both lysoNa$_V$ and TPC1 currents (I_{TPC1}) lacked inactivation, even when recorded with a long (10 s) depolarization pulse (**Supplementary Fig. 3**). Finally, $I_{lysoNav}$ was abolished in the cardiac myocyte endolysosomes from *tpc* knockout mice. Transfecting TPC1 cDNA into the mutant cardiac myocytes rescued and markedly increased $I_{lysoNav}$ (**Supplementary Fig. 4**). These data indicate that lysoNa$_V$ is formed by TPC1.

TPC1 is found in all vertebrates and is conserved between human and mouse (91% sequence identity and 95% similarity)[37]. Similar to human TPC1, mouse TPC1 generated high-density lysoNa$_V$-like currents when transfected into HEK293T cells (12.3 ± 4.0 mA cm^{-2}, $n = 5$, assuming recorded organelle was a sphere with a diameter of 3 μm; **Supplementary Fig. 5**).

TPC1 and lysoNa$_V$ have similar PI(3,5)P2 sensitivity

We further compared the properties of the native endolysosomal $I_{lysoNaV}$ in cardiac myocytes and I_{TPC1} in TPC1-tranfected HEK293T cells. PI(3,5)P2 potentiates several plasma membrane and endolysosomal ion channels, including transient receptor potential channels (TRPs) and TPCs[19,38,39]. The sensitivity of the native cardiac lyso$_{NaV}$ and that of TPC1 were comparable (**Supplementary Fig. 6a**). Neither lysoNa$_V$ nor TPC1 were activated by PI(4,5)P2 or PI(3,4)P2 (**Supplementary Fig. 6b,c**). In addition, the voltage dependence of TPC1 was not affected by the concentration of PI(3,5)P2, suggesting that the channel's voltage dependence was not conferred by the lipid (**Supplementary Fig. 6d–f**).

TPC1 and lysoNa$_V$ are both activated by alkaline pH

TPC1 is widely expressed along the endolysosomal pathway[10]. It is known that the luminal pH of these organelles varies substantially as they mature and fuse with each other, ranging from approximately 6.5 in the early endosomes to approximately 4.5 in lysosomes[40,41], but how the organelles sense and control the pH is not well understood. Increasing luminal pH by one unit from 4.6 to 5.6 substantially shifted the conductance (G)-Ψ relationship of TPC1 toward hyperpolarization by 63 mV (**Fig. 3a–c**; at pH 4.6, $\Psi_{1/2} = 91.2 \pm 11.8$ mV, $\kappa = 28.7 \pm 5.4$ mV, $n = 6$; at pH 5.6, $\Psi_{1/2} = 28.2 \pm 7.0$ mV, $\kappa = 27.5 \pm 2.2$ mV, $n = 7$; at pH 6.6, $\Psi_{1/2} = 2.6 \pm 12.6$ mV, $\kappa = 48.9 \pm 3.5$ mV, $n = 5$). Similarly, lyso$_{NaV}$ from cardiac myocytes was highly pH sensitive, and its G-Ψ relationship was shifted by 62 mV upon a one-unit change in pH (**Fig. 3d**; at pH 4.6, $\Psi_{1/2} = 74.5 \pm 9.5$ mV, $\kappa = 27.8 \pm 4.2$ mV, $n = 7$; at pH 5.6, $\Psi_{1/2} = 12.4 \pm 6.4$ mV, $\kappa = 23.6 \pm 1.1$ mV, $n = 4$). These data suggest that lysoNa$_V$ also functions as an organellar H^+ sensor and that higher pH, found in early endosomes and lysosomes, enables the channel to open over a wide voltage range (**Fig. 3a–g**).

Previous recordings using voltage ramp protocols found that TPCs are inhibited by cytosolic ATP[20]. ATP reduced I_{TPC1} amplitudes but did not change the normalized I-Ψ relationship (**Supplementary Fig. 7**), suggesting that, unlike luminal H^+, cytosolic ATP does not affect the voltage dependence of channel gating. Native lyso$_{NaV}$s from cardiac myocyte (**Supplementary Fig. 4**) and kidney cell endolysosomes (**Supplementary Fig. 2**) were also inhibited by ATP.

It has been proposed that NAADP activates Ca^{2+} release from lysosomes via TPCs[10–13]. In the absence of Mg^{2+}, NAADP was shown to activate ~10% of the maximum endolysosomal TPC2-mediated Na^+ current[16]. Under our recording conditions, NAADP did not have obvious effects on the amplitudes or voltage dependence of I_{TPC1} (**Supplementary Fig. 8**).

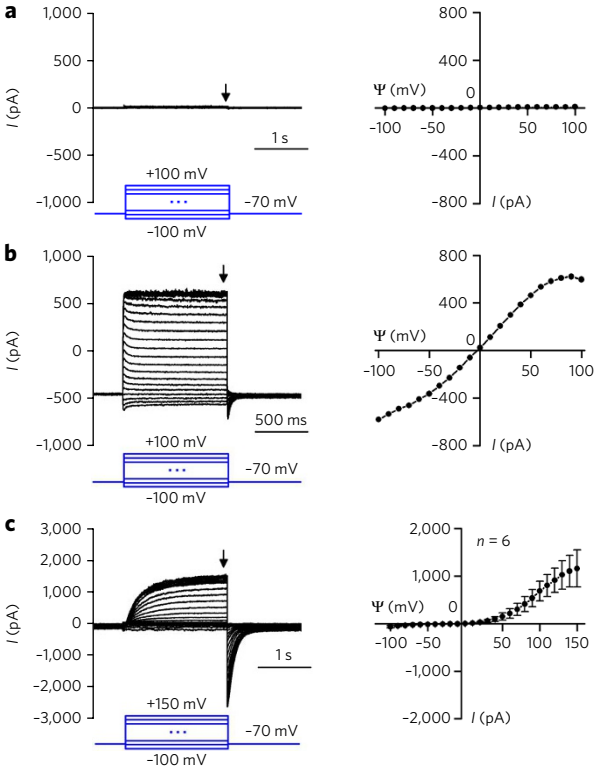

Figure 2 | TPC1, but not TPC2, forms a lysoNa$_V$-like voltage-gated channel. (**a–c**) Whole endolysosomal currents were recorded using step protocols as illustrated in the left panels from nontransfected HEK293T cells (**a**; $n = 9$) and stable HEK293 cell lines expressing hTPC2 (**b**; $n = 7$) or hTPC1 (**c**). The amplitudes of the step currents (indicated by arrows; left) were used to reconstruct the I-Ψ curves (right). Pipette solution contained 145 mM NaCl, 5 mM KCl, 1 mM $MgCl_2$, 2 mM $CaCl_2$, 10 mM HEPES, 10 mM MES, 10 mM glucose, pH 4.6. The symmetrical [Na^+] bath contained 140 mM Na-gluconate, 5 mM NaOH, 4 mM KCl, 2 mM $MgCl_2$, 0.39 mM $CaCl_2$, 1 mM EGTA, 0.001 mM PI(3,5)P_2, 10 mM HEPES, pH 7.2. Data are represented as mean ± s.e.m.

TPC1 is a highly Na^+-selective voltage-gated channel

The sequence of TPC1 has similarity to that of Ca$_V$s, and TPC1 has been thought to form Ca^{2+} channels[8,10]. We measured the permeability of TPC1 to various ions. Replacing luminal cations with large ions (150 mM *N*-methyl-D-glucamine (NMDG)) abolished the inward tail currents (**Fig. 4a**). Replacing cytosolic Na^+ with K^+ (**Fig. 4b**), Ca^{2+} (**Fig. 4c**) or NMDG (**Fig. 4d**) eliminated the step currents (**Fig. 4b–e**), suggesting that Na^+ was the major permeant ion. In addition, $[Ca^{2+}]_{cyt}$ had no major effect on I_{TPC1} (**Supplementary Fig. 9**). TPC1's relative ion permeabilities, measured by reversal potentials under bi-ionic conditions (**Fig. 4f,g**), were 212.3 ± 26.6 (P_{Na}/P_{Ca}; $n = 5$) and 78.1 ± 10.7 (P_{Na}/P_K; $n = 6$). The relationship between I_{TPC1}'s reversal potentials and $[Na^+]_{cyt}$ produced a slope of −56 mV per decade (**Fig. 4h**), which was close to −58 mV, the value predicted for a pure Na^+ electrode. TPC1's Na^+ selectivity is comparable with or higher than those of the 1×6TM and 4×6TM Na$_V$s[4,42]. We conclude that TPC1s form a new family of voltage-gated Na^+-selective channels.

Notably, TPC1 was inhibited by the Ca$_V$ blockers verapamil (half-maximum inhibitory concentration (IC_{50}) = 23.1 μM) and

© 2014 Nature America, Inc. All rights reserved.

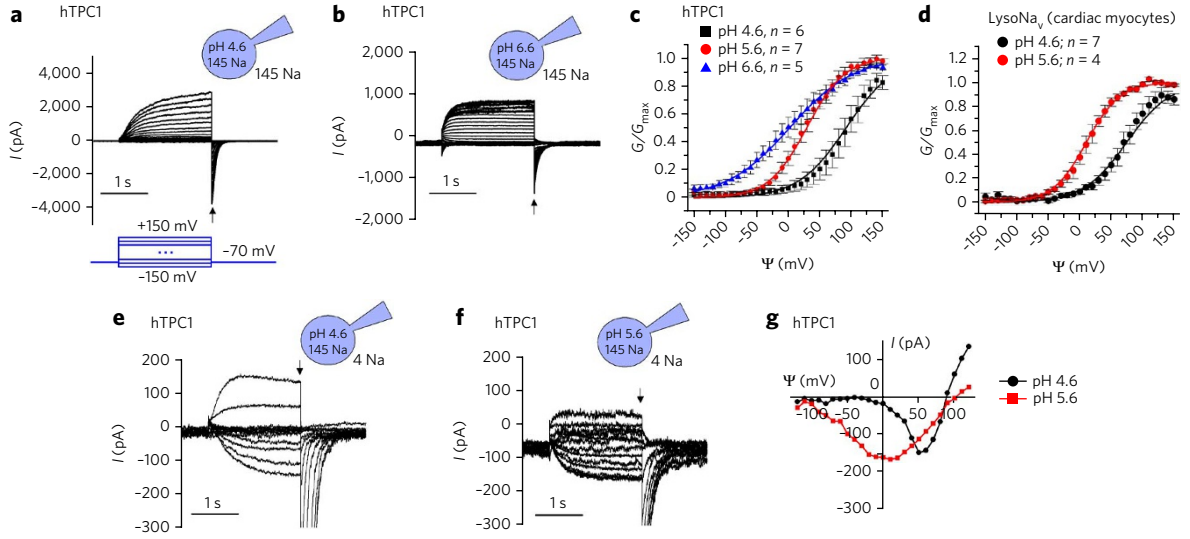

Figure 3 | Both lysoNa$_V$ and TPC1 are pH sensitive. (**a**–**g**) Whole endolysosomal currents were recorded using a step protocol as illustrated from hTPC1-expressing HEK293 cells or cardiac myocytes. Pipette solutions contained 145 mM NaCl, 5 mM KCl, 1 mM $MgCl_2$, 2 mM $CaCl_2$, 10 mM HEPES, 10 mM MES, 10 mM glucose and had a pH of 4.6, 5.6 or 6.6. In **a**–**d**, recordings were done with a symmetrical [Na^+] bath consisting of 140 mM Na-gluconate, 5 mM NaOH, 4 mM KCl, 2 mM $MgCl_2$, 0.39 mM $CaCl_2$, 1 mM EGTA, 0.001 mM PI(3,5)P_2 and 10 mM HEPES, pH 7.2. (**a**) Representative traces recorded with pH 4.6 pipette solution. (**b**) Representative traces recorded with pH 6.6 pipette solution. (**c**) Averaged G-Ψ relationships obtained from tail currents (at −70 mV, indicated by arrows in **a** and **b** and normalized to the extrapolated maximum; Online Methods) and fitted with Boltzmann equations. (**d**) Similar to **c**, but recorded from cardiac myocytes. (**e**–**g**) Recordings were performed under conditions with low $[Na^+]_{cytosol}$ with bath containing 140 mM K-gluconate, 5 mM KOH, 4 mM NaCl, 2 mM $MgCl_2$, 0.39 mM $CaCl_2$, 1 mM EGTA, 0.001 PI(3,5)P_2 and 10 mM HEPES, pH 7.2. Tail currents are truncated to resolve the step currents (indicated by arrows) used to reconstitute the I-Ψ curves. (**e**) Representative traces recorded with pH 4.6 pipette. (**f**) Representative traces recorded with pH 4.6 pipette. (**g**) I-Ψ relationships. Data are represented as mean ± s.e.m.

Cd^{2+} (IC_{50} = 180.2 μM; **Supplementary Fig. 10a–e**). Both I_{TPC1} and $I_{lysoNaV}$ were insensitive to the Na_V blocker TTX to concentrations up to 10 μM (**Supplementary Fig. 10e,f**), supporting the conclusion that lysoNa$_V$ is not formed by the TTX-sensitive 24TM proteins.

The S1-S4 domain functions as an organelle voltage sensor

How intracellular organelles detect voltage changes is not well understood. On the plasma membrane, the most well characterized voltage-sensing domains (VSDs) found in voltage-gated

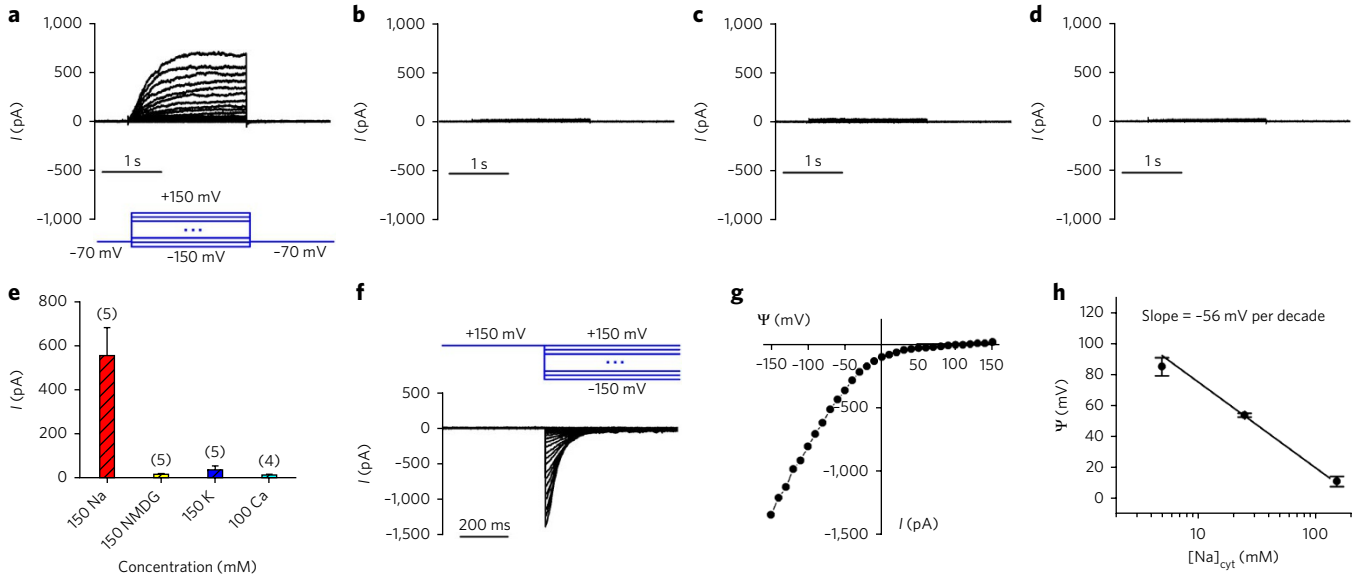

Figure 4 | TPC1 is Na$^+$ selective. I_{TPC1} was recorded from TPC1-expressing HEK293 cell endolysosomes with pipette solutions containing 5 mM HCl, 10 mM HEPES, 10 mM glucose, 10 mM MES (pH 4.6 with methanesulfonic acid) and 150 mM NMDG (**a**–**e**) or 150 NaOH (**f**–**h**). Bath solutions contained 150 mM NaCl (**a**), 150 mM KCl (**b**), 100 mM $CaCl_2$ (**c**), 150 mM NMDG-Cl (**d**) or other ions (**f**–**h**) as indicated (pH 7.2, buffered with 10 mM HEPES). Recordings in **a**–**e** used step protocols (−150 mV to +150 mV, 10 mV step, 2 s; illustrated in **a**). Notably, there was a reduction in inward tail currents, as shown in **a**. (**e**) Summary of I_{TPC1} amplitudes (at +150 mV) from **a**–**d**. (**f**) Tail currents elicited with a prepulse of +150 mV and measured at −150 mV to +150 mV (10 mV step, illustrated) with pipette solution containing 150 mM Na$^+$ and bath containing 100 mM Na^{2+}. (**g**) Amplitudes of tail currents from **f** were plotted against the test pulse voltages to determine the reversal potential. (**h**) Reverse potentials obtained with bath solutions containing varying [Na^+] and fitted with a linear function. Numbers of endolysosomes are in parentheses. Data are represented as mean ± s.e.m.

© 2014 Nature America, Inc. All rights reserved.

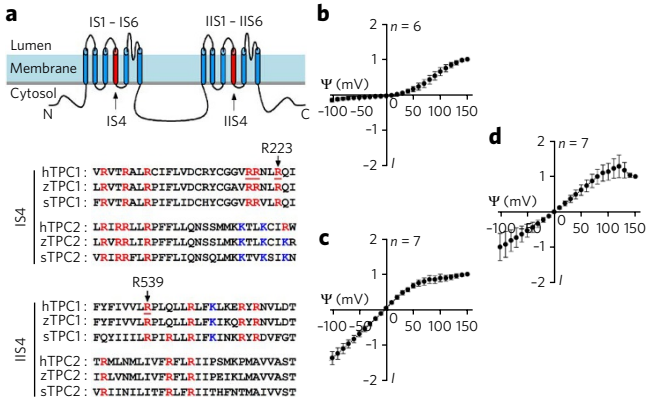

Figure 5 | Charged residues in the S4 domains contribute to the voltage-sensitivity of TPC1. (**a**) Top, TPC's 2×6TM membrane topology. Bottom, sequence alignment of putative IS4 and IIS4 regions of human (h), zebrafish (z), and sea urchin (s) TPCs. Residues R219, R220 and R223 in IS4 and residue R539 in IIS4 are underlined. (**b**–**d**) I-Ψ relationships (normalized to amplitudes obtained from +150 mV) of step currents recorded using symmetrical Na^+ conditions from wild-type hTPC1 (**b**) and hTPC1 with the R219Q R220Q R223Q mutations introduced in IS4 (**c**) or the R539I mutation introduced in IIS4 (**d**). Data in **b** were replotted from the recordings used in **Figure 2c** for comparison. Data are represented as mean ± s.e.m.

channels and voltage-sensitive enzymes[33,43–45] contain S1-S4 four-helix bundle structures with charged residues (lysine and arginine) at every third residue in S4. TPCs are the only predominantly endolysosome-localized proteins that contain two putative S1-S4 VSDs (IS4 and IIS4; **Fig. 5a**). Compared with the wild type (**Fig. 5b**), the TPC1 mutants with the charged residues in the first (**Fig. 5c**) or the second (**Fig. 5d**) S4 domain lost the voltage sensitivity. Thus, intracellular organelles use charged S1-S4 VSDs to detect changes in Ψ. Compared with the S4s of K_Vs, Na_Vs and Ca_Vs, the S4s of TPC1s are somewhat 'degenerated' and have fewer charged residues in the 'every third residue' manner (**Fig. 5a**). To determine how voltage change is sensed and coupled to TPC1 channel opening, more detailed studies are needed.

LysoNa$_V$ confers endolysosomal electrical excitability

On the plasma membrane of excitable cells, Na_V channels are fundamental in the generation of action potentials. We used current clamp experiments to test whether endolysosomes with lysoNa$_V$ currents were able to generate regenerative responses when electrically stimulated. In a subpopulation (6 out of 10) of endolysosomes from cardiac myocytes, a brief depolarizing current injection elicited spike-like depolarizing responses that lasted >2 s (**Fig. 6a**). The regenerative responses appeared to depend on I_{TPC1}, and those with responses had a larger I_{TPC1}-like current (364.7 ± 95.6 pA, n = 6, measured as the tail current amplitudes at −70 mV elicited by a depolarization to +150 mV; **Fig. 6a**) than those without responses (68.3 ± 8.3 pA, n = 4; **Fig. 6b**). Furthermore, depolarizing current injection did not elicit 'bi-stable' sustained responses in any of the endolysosomes from *tpc* knockouts (**Fig. 6c**; n = 12). Finally, depolarizing stimuli also elicited regenerative membrane potential responses in endolysosomes from TPC1-transfected HEK293 cells (5 out of 5) but not in the ones without TPC1 transfection (0 out of 6; **Supplementary Fig. 11**). Therefore, TPC1-mediated lysoNa$_V$ confers the electrical excitability of endolysosomes.

DISCUSSION

We have shown that endolysosomes are electrically excitable. The endolysosomal excitability depends on lysoNa$_V$, an atypical voltage-gated, noninactivating Na^+ channel. Luminal pH also gates the channel and controls excitability along the endosome-lysosome

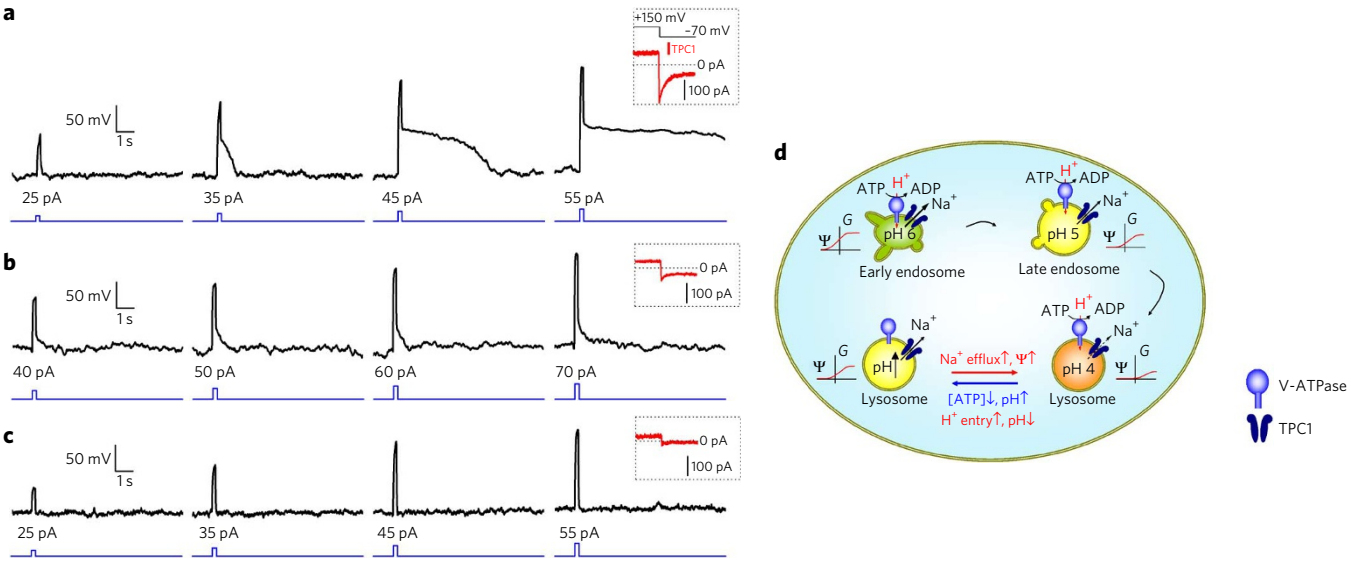

Figure 6 | TPC1 confers endolysosomal excitability. Current clamp recordings were performed using cardiac myocyte endolysosomes. The steady membrane potential of each endolysosome was first brought to −100 mV by current injection (Online Methods). A depolarizing current injection stimulus (200 ms, illustrated below each recording with size indicated) was then applied. The insets show the amplitude of the I_{TPC1}-like current (tail current at −70 mV elicited by the +150-mV pulse) recorded under voltage clamp from the same organelle with the same bath and pipette solutions used for current clamp experiments. (**a**–**c**) Representative Ψ responses in a wild-type endolysosome with a large I_{TPC1} (**a**), a wild-type endolysosome with a small I_{TPC1} (**b**) and an endolysosome from a *tpc* knockout (**c**). In **a**, stimuli above 35 pA elicited long-lasting depolarization. (**d**) A model illustrating the presumed roles of TPC1 in endolysosomal physiology. In endosomes where pH_{lumen} is high, TPC1 opens over a wide voltage range. In lysosomes where pH is low, TPC1 activity is low. During extracellular nutrient reduction, low intracellular ATP concentration or lysosomal alkalization increased TPC1 opening, leading to larger Na^+ effluxes and a more negatively charged lumen, which facilitates V-ATPase H^+ pumping, lumen acidification, proteolysis and nutrient production by lysosomes.

© 2014 Nature America, Inc. All rights reserved.

pathway. Our conclusion that TPC1 encodes lysoNa$_V$ is based on the following evidence: TPC1, but not the other TPC proteins, generates a lysoNa$_V$-like organelle Na$^+$ channel when it is heterologously expressed; TPC1 and lysoNa$_V$ are both insensitive to TTX and have similar phospholipid and ATP sensitivities; and lysoNa$_V$ is absent in the *tpc* knockout and is restored by TPC1 transfection. Whether the TTX-sensitive inactivating 4×6TM Na$_V$s, which are well characterized on the plasma membrane, also contribute substantially to voltage-activated Na$^+$ conductance in a subset of endolysosomes requires more extensive whole-organelle patch clamp studies[26]. With the discovery of TPC1 as part of a new voltage-gated Na$^+$ channel family, it is now clear that voltage-gated Na$^+$ channels can be formed by one[4], two (this study) and four repeats[5] of 6TM proteins, the three states during channel evolution from 6TM to 4×6TM.

On plasma membranes, the activation of K$_V$s and inactivation of Na$_V$s contribute the repolarization of action potentials[2]. The organelles we recorded do not seem to have K$_V$s. Conductance from CLCs may contribute to the falling phases of endolysosomal depolarization. Similarly, Na$^+$ efflux upon TPC opening may markedly lower $[Na^+]_{lumen}$ and the equilibrium potential for Na$^+$ because of the small sizes of the organelles. Further, more extensive studies are needed to monitor the luminal ionic concentrations and to determine the contribution of each ionic conductance to the dynamics of organelle membrane potentials under physiological conditions.

Unlike TPC1, TPC2 is voltage insensitive (**Fig. 2**) and presumably functions like a Na$^+$-leak channel in intracellular organelles. Similar functional distinctions between voltage-activated Na$_V$s and voltage-independent, Na$^+$-permeable leak channels exist on plasma membranes[46,47]. On the plasma membrane of neurons, a Na$^+$-leak channel, NALCN, which is a 4×6TM channel with sequence similarity to TPCs, regulates neuronal resting membrane potential[47]. On the endolysosomal membrane, the TPC2-mediated Na$^+$ leak channel, together with the K$^+$ leak and the other basal conductances we detected (**Supplementary Fig. 1**), most likely control resting Ψ and its responses to stimuli such as phospholipids, ATP and nutrients[19,20].

Na$_V$-mediated action potentials on the plasma membrane lead to depolarization-induced Ca^{2+} influxes in the nerve terminals and cardiac muscles by opening Ca$_V$ channels and to excitation-contraction coupling in skeletal muscle without requiring Ca^{2+} influx[48,49]. Whether a lysoNa$_V$-mediated depolarization spike on an endolysosomal membrane is able to increase $[Ca^{2+}]_{cyt}$ via voltage-activated Ca^{2+} efflux or control other processes such as organelle motility is not yet known.

TPC1 integrates inputs from H$^+$ concentration in the lumen, voltage across the organelle membrane, lipid composition on the membrane, cytosolic ATP concentration and nutrient availability outside the cell[19,20]. We speculate that falling metabolism and energy production results in lysosomal luminal alkalization and low cytoplasmic ATP concentration. These conditions increase the opening of TPC Na$^+$ channels and depolarize the lysosome. Depolarization decreases the proton motive force, favoring luminal acidification by the V-ATPase. This, in turn, speeds proteolytic degradation of lysosomal contents for use in energy production (**Fig. 6d**). In addition, the pH-TPC1 feedback loop may help determine the dynamics of luminal pH and contribute to endolysosomal functions such as amino acid export, wound repair and membrane fusion.

Received 31 January 2014; accepted 27 March 2014;
published online 28 April 2014

METHODS

Methods and any associated references are available in the online version of the paper.

References

1. Hille, B. *Ion Channels of Excitable Membranes* (Sunderland, MA, 2001).
2. Hodgkin, A.L. & Huxley, A.F. A quantitative description of membrane current and its application to conduction and excitation in nerve. *J. Physiol.* (*Lond.*) **117**, 500–544 (1952).
3. Yu, F.H. & Catterall, W.A. The VGL-chanome: a protein superfamily specialized for electrical signaling and ionic homeostasis. *Sci. STKE* **2004**, re15 (2004).
4. Ren, D. *et al.* A prokaryotic voltage-gated sodium channel. *Science* **294**, 2372–2375 (2001).
5. Noda, M. *et al.* Expression of functional sodium channels from cloned cDNA. *Nature* **322**, 826–828 (1986).
6. Catterall, W.A. Voltage-gated sodium channels at 60: structure, function and pathophysiology. *J. Physiol.* (*Lond.*) **590**, 2577–2589 (2012).
7. Clapham, D.E. & Garbers, D.L. International Union of Pharmacology. L. Nomenclature and structure-function relationships of CatSper and two-pore channels. *Pharmacol. Rev.* **57**, 451–454 (2005).
8. Ishibashi, K., Suzuki, M. & Imai, M. Molecular cloning of a novel form (two-repeat) protein related to voltage-gated sodium and calcium channels. *Biochem. Biophys. Res. Commun.* **270**, 370–376 (2000).
9. Cai, X. & Patel, S. Degeneration of an intracellular ion channel in the primate lineage by relaxation of selective constraints. *Mol. Biol. Evol.* **27**, 2352–2359 (2010).
10. Calcraft, P.J. *et al.* NAADP mobilizes calcium from acidic organelles through two-pore channels. *Nature* **459**, 596–600 (2009).
11. Brailoiu, E. *et al.* Essential requirement for two-pore channel 1 in NAADP-mediated calcium signaling. *J. Cell Biol.* **186**, 201–209 (2009).
12. Galione, A. NAADP receptors. *Cold Spring Harb. Perspect. Biol.* **3**, a004036 (2011).
13. Zong, X. *et al.* The two-pore channel TPCN2 mediates NAADP-dependent Ca^{2+}-release from lysosomal stores. *Pflugers Arch.* **458**, 891–899 (2009).
14. Rybalchenko, V. *et al.* Membrane potential regulates nicotinic acid adenine dinucleotide phosphate (NAADP) dependence of the pH- and Ca^{2+}-sensitive organellar two-pore channel TPC1. *J. Biol. Chem.* **287**, 20407–20416 (2012).
15. Schieder, M., Rotzer, K., Bruggemann, A., Biel, M. & Wahl-Schott, C. Planar patch clamp approach to characterize ionic currents from intact lysosomes. *Sci. Signal.* **3**, pl3 (2010).
16. Jha, A., Ahuja, M., Patel, S., Brailoiu, E. & Muallem, S. Convergent regulation of the lysosomal two-pore channel-2 by Mg^{2+}, NAADP, PI(3,5)P2 and multiple protein kinases. *EMBO J.* **33**, 501–511 (2014).
17. Lin-Moshier, Y. *et al.* Photoaffinity labeling of nicotinic acid adenine dinucleotide phosphate (NAADP) targets in mammalian cells. *J. Biol. Chem.* **287**, 2296–2307 (2012).
18. Walseth, T.F. *et al.* Photoaffinity labeling of high affinity nicotinic acid adenine dinucleotide phosphate (NAADP)-binding proteins in sea urchin egg. *J. Biol. Chem.* **287**, 2308–2315 (2012).
19. Wang, X. *et al.* TPC proteins are phosphoinositide-activated sodium-selective ion channels in endosomes and lysosomes. *Cell* **151**, 372–383 (2012).
20. Cang, C. *et al.* mTOR regulates lysosomal ATP-sensitive two-pore Na$^+$ channels to adapt to metabolic state. *Cell* **152**, 778–790 (2013).
21. Hilgemann, D.W., Feng, S. & Nasuhoglu, C. The complex and intriguing lives of PIP2 with ion channels and transporters. *Sci. STKE* **2011**, re19 (2001).
22. Suh, B.C. & Hille, B. PIP2 is a necessary cofactor for ion channel function: how and why? *Annu. Rev. Biophys.* **37**, 175–195 (2008).
23. Harikumar, P. & Reeves, J.P. The lysosomal proton pump is electrogenic. *J. Biol. Chem.* **258**, 10403–10410 (1983).
24. Steinberg, B.E., Touret, N., Vargas-Caballero, M. & Grinstein, S. *In situ* measurement of the electrical potential across the phagosomal membrane using FRET and its contribution to the proton-motive force. *Proc. Natl. Acad. Sci. USA* **104**, 9523–9528 (2007).
25. Stauber, T. & Jentsch, T.J. Chloride in vesicular trafficking and function. *Annu. Rev. Physiol.* **75**, 453–477 (2013).
26. Carrithers, M.D. *et al.* Expression of the voltage-gated sodium channel NaV1.5 in the macrophage late endosome regulates endosomal acidification. *J. Immunol.* **178**, 7822–7832 (2007).
27. Mindell, J.A. Lysosomal acidification mechanisms. *Annu. Rev. Physiol.* **74**, 69–86 (2012).
28. Saito, M., Hanson, P. & Schlesinger, P. Luminal chloride-dependent activation of endosome calcium channels: patch clamp study of enlarged endosomes. *J. Biol. Chem.* **282**, 27327–27333 (2007).
29. Dong, X.P. *et al.* The type IV mucolipidosis-associated protein TRPML1 is an endolysosomal iron release channel. *Nature* **455**, 992–996 (2008).
30. Cerny, J. *et al.* The small chemical vacuolin-1 inhibits Ca^{2+}-dependent lysosomal exocytosis but not cell resealing. *EMBO Rep.* **5**, 883–888 (2004).

© 2014 Nature America, Inc. All rights reserved.

31. Goldstein, S.A., Bockenhauer, D., O'Kelly, I. & Zilberberg, N. Potassium leak channels and the KCNK family of two-P-domain subunits. *Nat. Rev. Neurosci.* **2**, 175–184 (2001).
32. Decressac, S. *et al.* ARF6-dependent interaction of the TWIK1 K^+ channel with EFA6, a GDP/GTP exchange factor for ARF6. *EMBO Rep.* **5**, 1171–1175 (2004).
33. Jan, Y.N. & Jan, L.Y. Voltage-gated potassium channels and the diversity of electrical signaling. *J. Physiol.* (*Lond.*) **590**, 2592–2599 (2012).
34. Accardi, A. & Miller, C. Secondary active transport mediated by a prokaryotic homologue of ClC Cl cahnnels. *Nature* **427**, 803–807 (2004).
35. Leisle, L., Ludwig, C.F., Wagner, F.A., Jentsch, T.J. & Stauber, T. ClC-7 is a slowly voltage-gated $2Cl^-/1H^+$-exchanger and requires Ostm1 for transport activity. *EMBO J.* **30**, 2140–2152 (2011).
36. Schieder, M., Rotzer, K., Bruggemann, A., Biel, M. & Wahl-Schott, C.A. Characterization of two-pore channel 2 (TPCN2)-mediated Ca^{2+} currents in isolated lysosomes. *J. Biol. Chem.* **285**, 21219–21222 (2010).
37. Zhu, M.X. *et al.* Calcium signaling via two-pore channels: local or global, that is the question. *Am. J. Physiol. Cell Physiol.* **298**, C430–C441 (2010).
38. Zhang, Z., Okawa, H., Wang, Y. & Liman, E.R. Phosphatidylinositol 4,5-bisphosphate rescues TRPM4 channels from desensitization. *J. Biol. Chem.* **280**, 39185–39192 (2005).
39. Dong, X.P. *et al.* PI(3,5)P2 controls membrane trafficking by direct activation of mucolipin Ca^{2+} release channels in the endolysosome. *Nat. Commun.* **1**, 38 (2010).
40. Haggie, P.M. & Verkman, A.S. Defective organellar acidification as a cause of cystic fibrosis lung disease: reexamination of a recurring hypothesis. *Am. J. Physiol. Lung Cell. Mol. Physiol.* **296**, L859–L867 (2009).
41. Morgan, A.J., Platt, F.M., Lloyd-Evans, E. & Galione, A. Molecular mechanisms of endolysosomal Ca^{2+} signalling in health and disease. *Biochem. J.* **439**, 349–374 (2011).
42. Sun, Y.M., Favre, I., Schild, L. & Moczydlowski, E. On the structural basis for size-selective permeation of organic cations through the voltage-gated sodium channel. Effect of alanine mutations at the DEKA locus on selectivity, inhibition by Ca^{2+} and H^+, and molecular sieving. *J. Gen. Physiol.* **110**, 693–715 (1997).
43. Long, S.B., Tao, X., Campbell, E.B. & MacKinnon, R. Atomic structure of a voltage-dependent K^+ channel in a lipid membrane-like environment. *Nature* **450**, 376–382 (2007).
44. Bezanilla, F. How membrane proteins sense voltage. *Nat. Rev. Mol. Cell Biol.* **9**, 323–332 (2008).
45. Murata, Y., Iwasaki, H., Sasaki, M., Inaba, K. & Okamura, Y. Phosphoinositide phosphatase activity coupled to an intrinsic voltage sensor. *Nature* **435**, 1239–1243 (2005).
46. Crill, W.E. Persistent sodium current in mammalian central neurons. *Annu. Rev. Physiol.* **58**, 349–362 (1996).
47. Ren, D. Sodium leak channels in neuronal excitability and rhythmic behaviors. *Neuron* **72**, 899–911 (2011).
48. Catterall, W.A. Voltage-gated calcium channels. *Cold Spring Harb. Perspect. Biol.* **3**, a003947 (2011).
49. Beam, K.G. & Franzini-Armstrong, C. Functional and structural approaches to the study of excitation-contraction coupling. *Methods Cell Biol.* **52**, 283–306 (1997).
50. Bertl, A. *et al.* Electrical measurements on endomembranes. *Science* **258**, 873–874 (1992).

Acknowledgments

We thank members of the Ren lab for discussion and support and D. Clapham for suggestions. This work was funded, in part, by the American Heart Association, the US National Institutes of Health (grants 2R01NS055293 and 5R01NS074257 to D.R.) and the University of Pennsylvania Research Foundation.

Author contributions

C.C. developed the hypothesis that TPC1 is a depolarization-activated Na^+ channel and contributed all of the patch-clamp recording data, and C.C. and D.R. designed the experiments. D.R. supervised the research, B.B. and D.R. developed the cDNA constructs and the mouse model, and C.C. and D.R. wrote the manuscript.

Competing financial interests

The authors declare no competing financial interests.

Additional information

Supplementary information is available in the online version of the paper. Reprints and permissions information is available online at http://www.nature.com/reprints/index.html. Correspondence and requests for materials should be addressed to C.C. or D.R.

© 2014 Nature America, Inc. All rights reserved.

ONLINE METHODS

Animals and cell culture. Animal protocols were approved by the IACUC committee at the University of Pennsylvania. The generation of *tpc* knockout mice (with *tpc1* and *tpc2* disrupted) was previously described[20].

Cells were cultured in a humidified CO_2 (5%) incubator at 37 °C. HEK293T cells were cultured in DMEM (Gibco) supplemented with 10% FBS (Lonza) and 1× GlutaMax (Gibco) and were transfected using Lipofectamine 2000 (Invitrogen). Mouse TPC1 (C-terminally GFP tagged, in vector pEGFP-N1) was used in **Supplementary Figures 4** and **5**, and human TPCs (hTPC1 and hTPC2) were used in the other studies. Stable, Flp-In T-Rex-293 cell lines expressing hTPC1 and hTPC2 were generated by transfecting cDNA constructs (in vector pcDNA5/FRT/TO) encoding C-terminally GFP-tagged TPCs. Expression was induced with doxycycline (1 μg/ml for 48–72 h). Mouse inner medullary collecting duct kidney (mIMCD3) cells and cardiac myocytes were cultured in DMEM/F12 (Gibco) supplemented with 10% FBS and 1× Penicillin-Streptomycin. Cardiac myocytes were isolated from neonatal mice within 1 week of birth. Hearts were quickly excised and immersed in ice-cold HBSS (Gibco). Ventricles were cut into small pieces and digested by shaking at 250 r.p.m. for 5 min at 37 °C in HBSS containing 0.08% (w/v) collagenase (type II, Worthington) and 1% BSA (Sigma-Aldrich). After digestion, 10% FBS was added to stop the enzyme reaction. The mixture was pipetted up and down several times to disperse the cells, and then spun at 800 r.p.m. (82*g*) for 5 min at 4 °C. Cells were resuspended in culture medium and plated on coverslips. Peritoneal macrophages were extracted from adult mice (3–4 months old) by injecting 10 ml ice-cold PBS into the peritoneal cavity. Cells were cultured on coverslips in DMEM supplemented with 20% FBS and 1× penicillin-streptomycin as previously described[20].

Electrophysiology. Whole-endolysosome recordings were performed as previously described[20,28,29]. Macrophages and HEK293T and mIMCD3 cells were treated with 1 μM vacuolin-1 for 1–6 h and overnight, respectively, and cardiac myocytes were treated with 5 μM vacuolin-1 overnight. Recordings were performed using a Multiclamp 700B amplifier, a Digidata 1440A data acquisition system and pCLAMP software (Molecular Device). Recording pipettes made from borosilicate glass tubes were polished and had a resistance of 4–8 MΩ. Liquid junction potential was corrected, and agar salt bridge reference electrodes were used in recordings in which bath Cl^- concentration was changed.

Unless otherwise indicated in the figure legends, the standard symmetrical Na^+ bath solution used to record I_{TPC} and $I_{lysoNaV}$ with voltage clamping in **Figures 2**, **3a–d** and **5** and **Supplementary Figures 3** and **5–9** contained 140 mM Na-gluconate, 5 mM NaOH, 4 mM KCl, 2 mM $MgCl_2$, 0.39 mM $CaCl_2$, 1 mM EGTA and mM 10 HEPES (pH 7.2). Pipette solutions contained 145 mM NaCl, 5 mM KCl, 1 mM $MgCl_2$, 2 mM $CaCl_2$, 10 mM glucose, 10 mM HEPES and 10 mM MES (pH 4.6, adjusted with HCl). For Na^+ channel recordings, 1 μM $PI(3,5)P_2$ (or unless otherwise stated) was added to the bath to promote robust recordings and prevent channel rundown[19,20]. All of the lipids were in a water-soluble diC8 form (from Echelon Biosciences). For recordings presented in **Supplementary Figures 2**, **4** and **10**, the bath solution contained 150 mM NaCl and 10 mM HEPES (pH 7.2, adjusted with NMDG), and the pipette solution contained 145 mM Na-methanesulfonate, 5 mM NaCl, 10 mM glucose, 10 mM MES and 10 mM HEPES (pH 4.6, adjusted with methanesulfonic acid).

The relative permeability of TPC1 (**Fig. 4**) was calculated using the following equations:

$$P_K/P_{Na} = [Na]_{lumen} \exp(-\Psi_{rev}F/RT)/[K]_{cytosol} \quad (1)$$

$$P_{Ca}/P_{Na} = \{[Na]_{lumen} \exp(-\Psi_{rev}F/RT)\,[\exp(-\Psi_{rev}F/RT) + 1]\}/\{4[Ca]_{cytosol}\} \quad (2)$$

where Ψ_{rev} is the reverse potential measured with tail currents, F is Faraday's constant, R is the gas constant, and T is the absolute temperature. The voltage dependence of channel activation was studied with voltage-step protocols using bath and pipette solutions containing 145 mM or 150 mM Na^+ as indicated in the figures.

Whole endolysosomal inward I_{TPC1} has also been previously recorded with solutions with asymmetric Na^+ concentrations (145 mM luminal and 4 mM cytosol)[19,20] and ramp protocols (between +100 and −100 mV[20]). Those recording conditions favored inward currents but were not ideal for revealing TPC1's voltage dependence because of the channel's high voltage threshold of activation and slow deactivation. As such, some of the previous TPC1 currents recorded with ramp protocols were likely mixed with 'tail' currents.

To obtain the activation curves in **Figure 3c**,**d**, the amplitudes of the tail currents recorded from endolysosomes were fitted with Boltzmann equations to obtain the extrapolated I_{max}, half maximum activation voltage $\Psi_{1/2}$ and slope factor κ values. The G/G_{max} (calculated as I/I_{max}) values of all the recordings were then averaged and fit to the Boltzmann equation.

$$G/G_{max} = 1/(1 + \exp[(\Psi_{1/2} - \Psi)/\kappa]) \quad (3)$$

The inhibition curves presented in **Supplementary Figure 10b**,**d** were fitted with the equation:

$$I/I_0 = 1/[1 + (X/IC_{50})^h] \quad (4)$$

where I and I_0 are the currents obtained in the presence and absence of blockers, respectively, X is the blocker concentration, IC_{50} is the concentration required for half-maximal inhibition and h is the Hill coefficient.

To determine the relative Na^+ (P_{Na}/P_K) and H^+ (P_H/P_K) permeability of whole endolysosomes from macrophages, current-clamp recordings were performed using a pipette solution containing 150 mM NMDG, 1 mM HCl, 1 mM EGTA and 10 mM MES (pH 4.6, adjusted with methanesulfonic acid). Resting potentials were obtained using three different bath solutions containing 1 mM HCl, 1 mM EGTA, 10 mM HEPES (pH 7.2, adjusted with methanesulfonic acid or NMDG) and 150 mM K-methanesulfonate (bath 1), 150 mM KCl (bath 2) or 150 mM Na-methanesulfonate (bath 3). Relative permeability was calculated with the three resting potentials (Ψ) using the Goldman-Hodgkin-Katz equation:

$$\exp(\Psi F/RT) = (P_K[K^+]_{lumen} + P_{Na}[Na^+]_{lumen} + P_H[H^+]_{lumen} + P_{Cl}[Cl^-]_{cytosol})/ (P_K[K^+]_{cytosol} + P_{Na}[Na^+]_{cytosol} + P_H[H^+]_{cytosol} + P_{Cl}[Cl^-]_{lumen}) \quad (5)$$

For current-clamp recordings presented in **Figure 6** and **Supplementary Figure 11**, the bath solution contained 140 mM K-gluconate, 4 mM NaCl, 2 mM $MgCl_2$, 0.39 mM $CaCl_2$, 1 mM EGTA, 0.001 mM $PI(3,5)P_2$ and 10 mM HEPES, pH 7.2. The pipette solution contained (in mM) 70 mM KCl, 70 mM Na-methanesulfonate, 1 mM $MgCl_2$, 2 mM $CaCl_2$, 10 mM HEPES, 10 mM glucose and 10 mM MES, pH 5.5. Hyperpolarizing current was injected to bring the resting Ψ of each endolysosome to −100 mV to inactivate TPC1 (Ψ was less stable at −70 mV for unknown reasons). A current pulse (200 ms) with the indicated size was injected to elicit depolarization.

Data analysis. Data was analyzed and plotted using Clampfit (Molecular Device), Origin (Origin Lab) and Excel (Microsoft). Data are shown as mean ± s.e.m. Student's *t*-test and the Mann-Whitney rank sum test were used to compare between two groups.

© 2014 Nature America, Inc. All rights reserved.

doi:10.1038/nchembio.1522